ARCHITECTURAL COMPARISON OF ADVANCED ULTRA-HIGH BYPASS RATIO TURBOFANS FOR MEDIUM TO LONG RANGE APPLICATION

J. Bijewitz, A. Seitz and M. Hornung,
Bauhaus Luftfahrt e.V., Deutschland

Abstract

The ambitious long-term environmental objectives for aviation recently announced by the European Commission stipulate significant efficiency improvements for aircraft and their propulsion systems. In view of this, the exploration of radical and unconventional propulsion system design solutions is necessary. In order to ensure an appropriate assessment of such highly advanced unconventional propulsion system concepts, consistent benchmarking against conventional power plant architectures featuring similarly advanced technology status is required. This paper focuses on the comparison of two different types of evolutionary improved Ultra-High Bypass Ratio turbofan engines that may be considered as reference technology benchmarks for a potential wide-body, medium to long range application (4800 nm, 340 passengers) with an entry-into-service year of 2035+. These include a direct drive three-spool design as well as a two-spool geared architecture. After having presented design laws implemented in a gas turbine performance software, several parametric design studies are employed for both engine layouts allowing for the identification of suitable design points, both for the isolated propulsion system and under consideration of first order vehicular cascade effects.

1. INTRODUCTION

The ambitious long-term emission reduction targets for aviation recently unveiled by the European Commission [1] require substantial improvements in aircraft energy efficiency. Thus, apart from the improvement of power plant efficiency itself also the enhancement of vehicular efficiency e.g. through introduction of synergistic propulsion system integration concepts utilizing Distributed Propulsion [2] and adaptive nacelle solutions [3] is currently being fundamentally investigated in European research projects. Large-scale research activities targeting a reduction of gas turbine fuel consumption have been focusing on enhancing thermal efficiency through advanced core engine technologies [4], as well as propulsive efficiency by introducing innovative low-pressure systems [5]. Concurrently, research on advanced engine subsystem components is being conducted [6]. Efficiency gains have been predicted by the introduction of highly advanced cycles improving components such as hybrid energy propulsion concepts [7]. In order to ensure consistent benchmarking, it is required to compare these radical technology concepts against similarly advanced but rather conventional propulsion system options potentially available in the same timeframe. In this respect, efficiency increases still can be expected from the incremental improvement of the conventional Joule/Brayton cycle and especially from extensive exploitation of Ultra-High Bypass Ratio (UHBPR) turbofans. As the gas turbine based engine will be the dominant power plant architecture in the foreseeable future, this paper focuses on the comparative evaluation of the characteristics of two different types of evolutionary improved UHBPR engines targeting an entry-into-service year of 2035+.

While the improvement of thermal efficiency becomes increasingly limited by feasible temperature and pressure levels, and, moreover, component efficiencies have already reached very high levels, a key to further overall efficiency gains is rooted in the improvement of propulsive efficiency. Here, the main driver is the reduction of the ratio of mean nozzle exit and free stream velocity. A low fan nozzle exit velocity is generally obtained by reducing fan pressure ratio, which requires for maintaining a certain net thrust an increase of fan diameter. This is typically realized by increments of engine bypass ratio, i.e. the amount of mass flow passing through the bypass duct relative to the core engine flow. While the performance of the power plant itself can be improved through this measure in terms of specific fuel consumption (SFC), engine weight and drag increase simultaneously, thereby penalizing the attainable fuel efficiency improvement. Moreover, the feasible fan diameter is often constrained by parameters associated with power plant installation such as the minimum permissible nacelle ground clearance and nose wheel collapse scenarios. Therefore, the selection of optimum bypass ratio at vehicular level is a complex trade-off involving engine and aircraft-related design parameters.

The introduction of a gear system between the low pressure turbine and the fan is considered a key enabler for UHBPR. Therefore, a number of comparative studies between advanced Geared Turbofan (GTF) and Direct Drive Turbofan (DDTF) engine architectures can be found in the literature (e.g. [8], [9]). While Kurzke [8] and Larsson et al. [9] compared the characteristics of a GTF with those of a two-spool DDTF for short range application, the present paper seeks to investigate if similar design rules apply for a different market segment and an alternative DDTF architecture. Hence, this analysis will focus on the comparison of an advanced two-spool GTF and a three-spool DDTF both utilizing UHBPR and powering a medium to long range twin-engine aircraft for a year 2035+ entry-into-service (EIS) scenario.

After discussing the modeling approach as well as imposed design heuristics, parametric design studies will be performed in order to compare and contrast both engine options, and hence to identify design trends and optimum design points, both for the isolated propulsion system and under consideration of cascade effects at vehicular level.

2. SYSTEM MODELING

This section initially provides an overview of the application scenario targeted with the present investigation. In addition, the general architectural differences between the selected power plant options are highlighted. After describing the modeling approach and implemented design laws, settings and assumptions for turbine cooling air mapping and component efficiency assessment are discussed.

2.1. Application Scenario and Overview of Investigated Engine Architectures

In a previous investigation [10] a parametric model for an Airbus A330-300 equipped with Rolls-Royce Trent 700 engines representing a typical year 2000 technology status had been fashioned. For the design studies performed in the present context the investigated power plants were considered to be applied to a potential successor, an evolutionary improved medium to long range twin-engine aircraft. In the conceptual investigation described in Reference [10] the design range had been selected as 4800 nm while accommodating a design payload of 340 passengers. Flight Mach number for Long Range Cruise was M0.80. In view of a 2035+ EIS, technology freeze was declared as 2030 and a set of aerodynamic and weights reduction related technologies appropriate for the targeted timeframe was implemented. These included an advanced flexible wing with an aspect ratio of 12.6. With regards to structural design, omni-directional ply orientation of carbon fibers and advanced bonding techniques were assumed to be available [10]. As a consequence, the sizing thrust requirement of the advanced aircraft was found to be approximately 17% below the value of the year 2000 system.

Two different advanced aero engine architectures were considered feasible for an ultra-high bypass ratio turbofan engine in the 300 kN (~70 000 lbf) thrust class: On the one hand, a direct-drive three-spool turbofan and on the other hand, a two-spool boosted geared turbofan. While the DDTF features a separate spool for the intermediate pressure system and thus provides improved flexibility regarding the speed selection of the Intermediate Pressure Compressor (IPC) and Intermediate Pressure Turbine (IPT) than a classic 2-spool direct drive turbofan, the GTF utilizes a fan drive gear system intended to decouple the speed of the fan and the low pressure spool. In view of the considered thrust class and expected large fan diameters, both architectures were assumed to feature a Short Duct Separate Flow (SDSF) nozzle design.

2.2. Modeling Approach

Since engine sizing thrust requirement is, amongst others, dependent on aircraft Maximum Take-off Weight (which is influenced by the propulsion system weight) and the aerodynamic efficiency of the aircraft (which is mainly affected by the nacelle wetted area, in the first instance), integrated propulsion system and aircraft sizing generally is an iterative effort. However, as the analysis described in the present context is intended to focus on the propulsion system related aspects, the investigation was performed under the assumption of a fixed sizing thrust requirement. Further key assumptions with respect to propulsion system design are summarized below:

- Acknowledging the 2035+ EIS, the aircraft was assumed to be equipped with an all-electrical systems architecture [10]. Thus, a zero off-take scenario with regards to customer bleed air and mechanical power extraction was assumed.
- Typical turbo component hub to tip ratios and axial Mach numbers according to Reference [11] were applied.
- Requirements associated with cooling of the fan drive gear system of the GTF were neglected.

As a modeling environment for sizing and performance studies, GasTurb11® [12] was utilized and off-design calculations were based on standard component maps. Propulsion system sizing was conducted at Top-of-Climb (TOC) conditions (Mach 0.78, FL350) with Maximum Climb (MCL) thrust setting, since highest corrected mass flows typically occur at that operating condition, thereby constituting the relevant condition for flow path sizing. Plausibility of the results was checked during performance calculations by verifying that temperatures and spool speeds were within feasible ranges at hot day take-off condition. The main specifications at sizing point applied for both engine configurations are summarized in TAB 1.

TAB 1: Propulsion system specifications at flow path sizing point

Property	Value
Propulsion system sizing point	Top-of-Climb M0.78, FL350, ISA
Thrust setting	Maximum Climb (MCL) thrust
Net thrust	56.0 kN

For reasons of geometric limitation in a single-stage planetary gearbox, a gear ratio of 4.5 of the fan drive gear system was assumed as an upper bound for the GTF throughout the investigations. Maximum allowable temperature levels typically occurring at take-off condition were prescribed according to the advanced technology level considered in the present study and restricted as given in TAB 2. The maximum Low Pressure Turbine (LPT) inlet temperature T_{45} was selected in order to allow for an uncooled LPT. The number of LPT stages was limited to 9 throughout the analyses, which was considered an upper practical limit regarding part count, complexity and maintenance effort, cf. References [8], [13]. The final constraint refers to the structural integrity metric AN^2 constituting the product of a turbo component's annular area and rotational speed.

TAB 2: Assumed limits for propulsion system sizing

Assumed Limit	Max. Value
Gear Ratio [a]	4.5
LPT stage count	9
HPC exit temperature T_3	1000 K
HPT inlet temperature T_4	2050 K
LPT inlet temperature T_{45}	1350 K
AN^2 @ LPT exit	13000 m²/s²

[a] only applicable for GTF

A generic fuel with a lower heating value of 42.8 MJ/kg was used. In order to reflect similar technological settings of the engine architectures, both options were subsequently compared at identical Overall Pressure

Ratios (OPR) and Turbine Entry Temperatures (TET). The specific values were subject to parametric studies and are presented in Section 3.

2.3. Implemented Design Laws

In order to enable a consistent treatment of both engine options and to allow for parametric studies, the turbofan design models were supplemented with an in-house developed set of iteration loops based on Reference [14]. These design heuristics included classical thrust sizing via control of engine inlet mass flow (W_2). The outer fan pressure ratio (p_{13}/p_2) was iteratively adjusted to yield the optimum ratio of flow velocities in the bypass and core nozzle jets (V_{18}/V_8) [15]. Fan tip speed was correlated with outer fan pressure ratio according to data given in Reference [11]. Compressor work split was selected in order to allow for uncooled LPTs. For the bypass nozzle discharge and core thrust coefficients, correlations depending on the nozzle pressure ratio for cold and hot nozzles according to Reference [14] based on empirical data given in [11] were incorporated.

2.4. Determination of Turbine Cooling Air Demand

For the determination of the required amount of turbine cooling air the method presented in Reference [14] was employed. Stators and rotors of both components were considered to be cooled by bleed air taken from the High Pressure Compressor (HPC). In order to yield appropriate temperature and pressure levels of the cooling air, the HPT cooling air was taken from the HPC exit, whereas the IPT cooling air was considered to be supplied from HPC inter-stage bleed. For the determination of the cooling air mass flow, $\dot{m}_c$, relative to the HPC inlet mass flow, $\dot{m}_{25}$, a relation from Reference [17] was used:

$$\frac{\dot{m}_c}{\dot{m}_{25}} = c_c \cdot \left(\frac{\eta_c}{1-\eta_c} \right) \tag{1}$$

where the cooling effectiveness η_c is defined as [16]:

$$\eta_c = \frac{T_{HG} - T_M}{T_{HG} - T_{CA}} \tag{2}$$

with T_{HG}, T_M and T_{CA} being the temperature of the working fluid at the considered turbine blade row, the bulk temperature of the blade material and the cooling air temperature, respectively. An empirical technology factor, c_c, was selected to reflect year 2030 technology level. While flow path sizing was performed at a top-of-climb condition with MCL thrust setting, maximum temperature levels occurring at take-off were used in equation (2) for the hot gas temperature and the cooling air temperature, respectively. As GasTurb11 uses an equivalent single-stage model, the calculation of two-stage cooled turbines requires a transformation. For that, the method for conversion of multi-stage cooled turbines to single-stage turbines described in Reference [14] was used and typical work potential assignments for each grid according to Reference [14] were implemented.

The used relations were subsequently implemented for the DDTF and the GTF. It was found that almost the same total cooling air demand is required for the DDTF and GTF, resulting from identical turbine inlet temperatures and OPRs as well as equal technology settings regarding cooling effectiveness and material properties.

2.5. Component Efficiency Assessment

Evolutionary turbo components were assumed for both the DDTF and the GTF. In the first instance, the design efficiency of each component may be considered a function of technology level, turbo component size and mean stage loading. While the first two aspects have a similar impact on both GTF and DDTF, the latter one differs for both of the engine architectures and each component. One of the main distinctions is rooted in the arrangement of the intermediate pressure system, which in case of the DDTF consists of a separate third shaft, compressor and turbine and in case of the GTF only of a booster driven by the LP spool. Moreover, the engine types employ significantly different design philosophies of the LPT leading to different stage loadings and design efficiencies.

Inner and outer fan, IPC/booster, HPC, HPT and IPT were assigned a specific design efficiency which was retained constant during the studies. The specific values depend on the selected stage configuration and are thus given in Section 3.4 (TAB 3). As the highest impact of turbo component efficiency on engine fuel consumption is typically associated with the LPT [14, Fig. A2], emphasis was placed on capturing the intrinsic architectural characteristics between the LPT designs of DDTF and GTF and translating these into the respective efficiency delta. For the mapping of LPT efficiency, a quadratic correlation was derived from the data given in Reference [11] exhibiting sensitivity to mean stage loading factor,

$$\psi_m = \frac{\Delta h}{n_{st} \cdot \left(U_m^2 / 2 \right)} \tag{3}$$

where Δh is the component total enthalpy change, n_{st} the LPT stage count and U_m represents the rotor blade velocity at representative mean diameter. Since from a noise, structural integrity and transonic efficiency point of view the fan tip speed restricts the speed of the LP shaft, the LPT of the DDTF is forced to rotate at a lower speed than desired, thus resulting in high stage loadings. Although employing more stages, the efficiency is typically degraded compared to the geared configuration.

For further components such as spools, intake, burner and ducts typical efficiencies and pressure ratios, respectively, were assumed.

3. CYCLE DESIGN AND SIZING APPROACH

In this section the approach for cycle design and engine sizing used for the present conceptual analysis is described. As part of this, parametric studies employed to identify the most feasible design point for both the DDTF and the GTF are presented.

3.1. OPR and TET Study

The objective of an initial study was the determination of an appropriate TET and OPR level. Therefore, these two parameters were varied in a two-dimensional parametric study with fixed BPR and net thrust at MCL conditions. The study was conducted for both engine options, and, as similar characteristics were obtained for both architectures, only the results corresponding to the GTF are discussed below.

Reynolds number and size effects were neglected for core size variations, in the first instance. The results for the GTF are summarized in BILD 1 where core efficiency is plotted versus the design TET ($T_{4,des}$) with OPR as a parameter. Additionally, contour lines indicate the relative amount of total required HPT cooling air. As can be seen from BILD 1, the lines of constant OPR only exhibit weak dependence from varying values of $T_{4,des}$ and are shifted towards higher core efficiencies with increasing values of OPR. As a plausibility check, consider the case of an ideal Joule cycle where core efficiency does not exhibit sensitivity to burner exit temperature and is only dependent on cycle pressure ratio [18]. The TETs, at which the respective maxima of η_c are reached, increase with rising OPRs. With the given study settings maximum core efficiency is identified to decrease again with OPRs in excess of approximately 65. The cooling air amount increases both with higher values of OPR and $T_{4,des}$ since higher OPRs imply higher cooling air temperatures, and higher values of $T_{4,des}$ lead to an increased hot gas temperature and thus high thermal loads of the turbine. Generally, the improvement potential achievable with an increase in OPR appears to be rather small with respect to core efficiency within the considered range of parameters. The maximum achievable benefit is only about 2.5%.

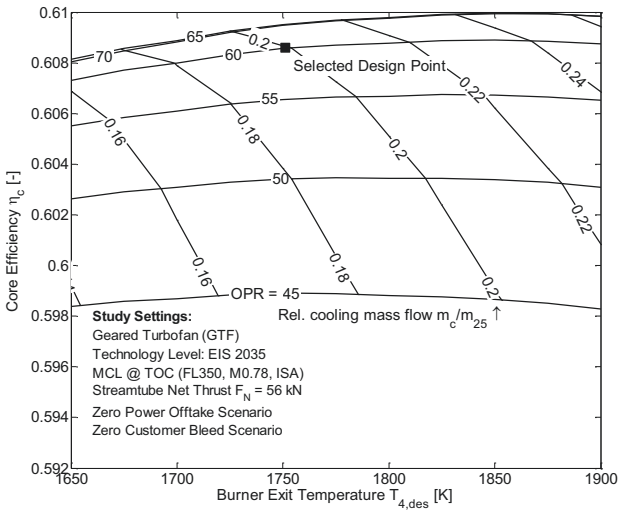

BILD 1: Study results for determination of design TET and OPR. Contours indicate OPR and relative total amount of cooling air

Therefore, a best and balanced approach for the selection of $T_{4,des}$ and OPR was chosen yielding a high efficiency level at TETs corresponding to feasible temperature levels at take-off condition. For OPR, a value of 60.0 was assumed. Applying even higher values of OPR would yield only insignificant benefits in terms of η_c, and exceed the allowable HPC exit temperature (T_3) at take-off. Although not explicitly mapped in this context, it might also yield very low blade heights in the last HPC stages, thus leading to larger relative gaps and manufacturing issues.

For the design burner exit temperature, a value of 1750 K was selected in order to stay within the limit of 2050 K during maximum take-off conditions. Despite higher cycle temperatures, the improved cooling and material technologies assumed for the targeted timeframe yield relative cooling mass flows of approximately 20%. These design settings were retained throughout the following design studies.

3.2. Direct Drive Turbofan (DDTF)

As outlined above, for the DDTF a three-spool unmixed flow architecture was assumed. Based on inspection of mean stage loadings and pressure ratios emanating from the cycle properties identified in the last subsection, the stage configuration was determined using design guidelines provided in Reference [11]. It was assumed that advances in compressor technology would allow for a moderately increased pressure ratio per stage and the ability to still allow for slight improvements in compressor efficiency relative to current technology. As a result of the studies presented later on in this section, this resulted in the same compressor stage configuration as implemented on the Trent XWB [19], namely an IPC stage count of 8 and a 6-stage HPC. A single stage HPT was assumed, whereas for the IPT 2 stages were required. The stage count of the LPT was subject to more detailed investigations described later in this section.

The basic schematic of a generic 3-spool separate flow turbofan is presented in BILD 2.

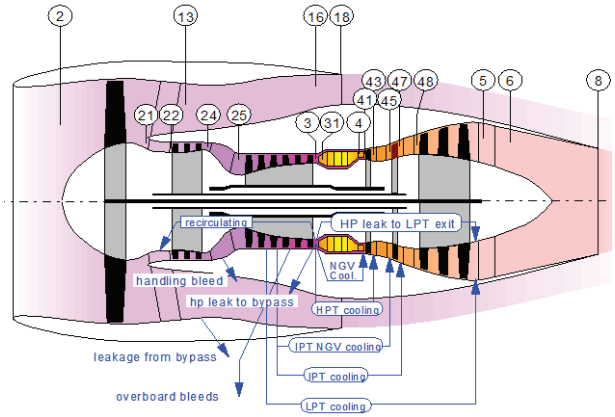

BILD 2: Generic three-spool Direct Drive Turbofan schematic [12]

In a subsequent study, the interrelations between SFC, fan tip diameter and turbo machinery stage count were investigated. For reasons of fuel efficiency and compliance with noise regulations, the design strategy of turbofans has recently been concentrated on realizing low jet velocity levels by decreasing fan pressure ratio, thereby improving propulsive efficiency. In order to maintain a certain net thrust, this requires higher engine inlet mass flows leading to an increased fan diameter. The typical challenge emanating from this design philosophy has been for the classic direct drive turbofan an increasing mismatch in rotational speed between LPT, booster and fan. For a feasible fan tip speed, higher BPR imply decreasing LP spool speeds requiring at constant LPT

loading a higher amount of stages, thus adding weight and complexity to the propulsion system. A further implication of lower rotational LP spool speeds is rooted in the increase of transmitted torque, resulting eventually in the requirement to increase the LP shaft diameter. While not explicitly modelled in the present context, this may constitute installation issues due to the requirement of fitting the LP shaft through the core spool.

The described context was investigated in a parametric design study where design Bypass Ratio BPR_{des} and net thrust (F_N) were varied at prescribed OPR and a fixed technological level. The study was conducted at a constant LPT mean stage loading of 5.5, hence yielding constant LPT efficiency, in the first instance. The resulting relations between fan inlet diameter and SFC improvement relative to year 2000 technology status are given in BILD 3 for varying values of net thrust, F_N, and BPR_{des}, where additionally the required LPT stage count is presented as dashed contour lines. As can be seen, at a given net thrust higher values of BPR_{des} lead to a decrease of SFC due to the improvement of propulsive efficiency. Simultaneously, the fan diameter increases with rising BPR, as a given thrust is produced with a lower velocity increment and hence higher total mass flow. As outlined above, larger fan diameters require more LPT stages at a constant mean stage loading. Although a very highly loaded LPT was assumed in the study, the upper range of considered BPR yields unrealistically high LPT stage counts. A change of net thrust at constant BPR_{des} requires variation of fan diameter and yields a constant level of SFC, thereby reflecting the assumption of the zero off-take scenario as well as negligible variations of component efficiency with engine size variation. The impact on the installed performance will further be discussed in Section 4.

3.3. Geared Turbofan (GTF)

Subsequently, a similar analysis was conducted for the GTF. Flow path sizing conditions and thrust setting were kept unchanged as given in TAB 1. A schematic view of a generic GTF is presented in BILD 4.

TET and OPR were selected identically as for the DDTF in order to represent the same core technology level. Regarding stage configuration, a similar assessment as for the DDTF was performed. Based on the evaluation of stage loading, feasible stage pressure ratios and adequate compressor work split it was found that the GTF required 9 stages for the HPC and a 2-stage HPT. For the booster, 3 stages were considered appropriate. The configuration of the LPT will be further discussed in Section 3.4.

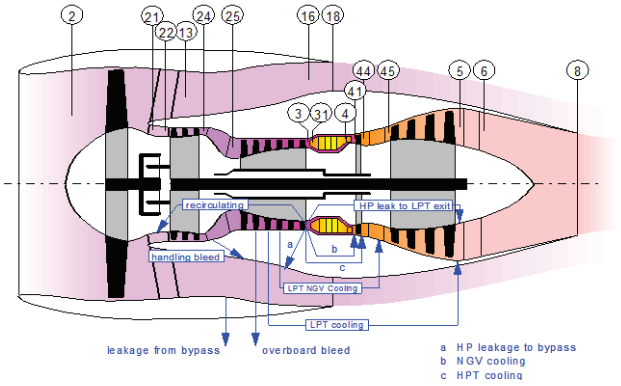

BILD 4: Generic two-spool Geared Turbofan schematic [12]

Similar to the DDTF, the impact of BPR on fan diameter and change of SFC was investigated. The respective chart is presented in BILD 3. By prescribing a fixed LPT speed at the representative mean diameter ($U_{LPT,m}$), the gear ratio of the fan drive gear system becomes an output parameter, which is also integrated in the figure using dashed contour lines. The value for $U_{LPT,m}$ was selected in a way that at Maximum Take-off (MTO) thrust setting the maximum permissible structural integrity metric AN^2 of about 13000 m²/s² (cf. Reference [11]) is not exceeded in the last LPT rotor. As can be seen, similar tendencies as for the DDTF are obtained.

3.4. Comparison of Power Plant Performance

Based on the selected stage configurations described in Sections 3.2 and 3.3, the turbo component design efficiencies were assessed. While the fan and HPC efficiency were evaluated to be approximately identical, the booster of the GTF was assumed to feature a slightly decreased efficiency considering increased mean stage loading. Following a similar rationale, the HPT of the GTF was expected to yield a 1.0 percentage point increased efficiency due to the 2-stage design. Compared to the

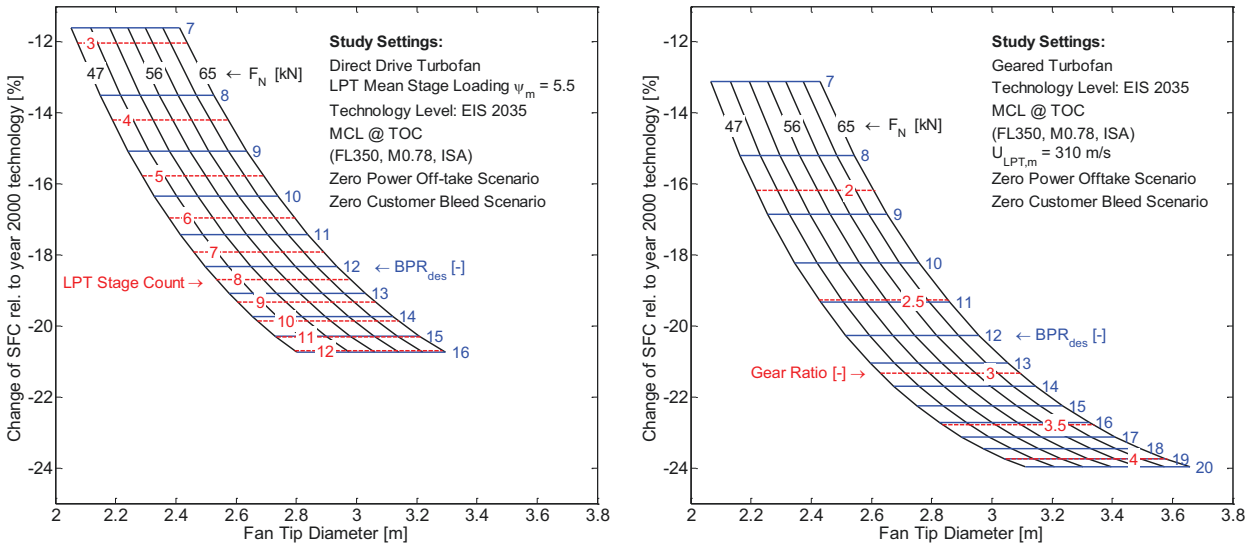

BILD 3: Relative design SFC and fan diameter as a function of design BPR and net thrust for DDTF and GTF designs

DDTF, the increased LP spool speed of the GTF causes the LPT stage loading to be reduced. A configuration with $\psi_m = 3.0$ yielding a 4-stage LPT design was considered an appropriate tradeoff between stage count and attainable efficiency benefit relative to the DDTF. As the loading is significantly reduced compared to the DDTF ($\psi_m = 5.1$), the LPT efficiency was assessed to be improved by 2.2 percentage points compared to the DDTF. TAB 3 summarizes the deltas in design efficiencies.

TAB 3: Estimated component design efficiency deltas

Component	Delta[a] [% points]
Polytropic outer LPC efficiency	±0.0
Polytropic inner LPC efficiency	±0.0
Polytropic booster or IPC efficiency	-0.5
Polytropic HPC efficiency	±0.0
Isentropic HPT efficiency	+1.0
Isentropic LPT efficiency	+2.2 [b]

[a] GTF relative to DDTF
[b] corresponds to design given in TAB 4

In BILD 5 the characteristics of the SFC improvement relative to year 2000 technology status resulting from the previous studies are presented for both the DDTF and the GTF for a given net thrust. In addition to varying design Bypass Ratio, also the impact of LPT stage count was analyzed for the DDTF. The resulting variation of LPT efficiency was correlated with LPT mean stage loading according to the approach described in Section 2.5. The obtained trends generally agree well with results published e.g. in Reference [20].

The characteristics of stage counts exceeding 9 stages are presented using dashed lines. As can be seen, under the given constraint of LPT stage count, minimum SFC for the DDTF is achieved using $BPR_{des} = 14.0$ and employing the maximum permissible number of LPT stages. The resulting SFC reaches a value of 13.27 g/s/kN. An insightful trend may be derived from BILD 5: For an increase of stage counts the optimum SFC of the DDTF decreases and its locus is shifted towards higher BPR. This is a direct result of the decreasing stage loading of the LPT, which correlates with improved LPT efficiencies. However, the relative gain decreases since the efficiency benefit becomes gradually smaller with lower stage loadings. Within the considered range of parameters the SFC of the GTF monotonically decreases and does not exhibit a stationary point – a characteristic, which is rooted in the ability of maintaining a high LPT efficiency by continuously increasing gear ratio with rising fan diameters. It should be noted that for BPR in excess of the values investigated in the present study SFC can be expected to rise again. This results from the increasing impact of pressure losses in the intake and bypass duct as fan pressure ratio decreases. However, as this yields fan diameters that were considered to be impractical, this range of BPR was excluded in the present context. The values for SFC of both engine options converge towards the lower end of BPR investigated which may be attributed to the LPT efficiency of the DDTF approaching the value of the GTF.

For defining a suitable point of comparison against the DDTF, the differential change of SFC with fan diameter (D_2), was derived from the trend for the GTF given in BILD 5. It was found that for fan diameters above 3.35 m the relative change of SFC dropped below 0.05% per centimeter increase in D_2. Hence, a fan diameter of 3.35 m was considered appropriate and the associated design features a BPR_{des} of 19.4 yielding a SFC of 12.67 g/s/kN. A synopsis of further design parameters corresponding to that particular design is provided in TAB 4.

As for constant flight conditions and energy sources SFC is inversely proportional to overall efficiency, the contributors to the SFC delta may conveniently be identified using an efficiency breakdown commonly used in gas turbine performance simulation [20]. In this respect, overall efficiency η_{ov} of the propulsion system may be split up into core efficiency, η_c, transmission efficiency, η_{tr} (where the product of η_c and η_{tr} constitutes thermal efficiency), and propulsive efficiency, η_{pr}. Hence, $\eta_{ov} = \eta_c \times \eta_{tr} \times \eta_{pr}$. As can be seen from TAB 4, the main share of the identified 4.5% relative improvement of SFC compared to the DDTF is rooted in the enhancement of propulsive efficiency due to the GTF's significantly reduced specific thrust level ($F_N/W_{2,des}$). The core

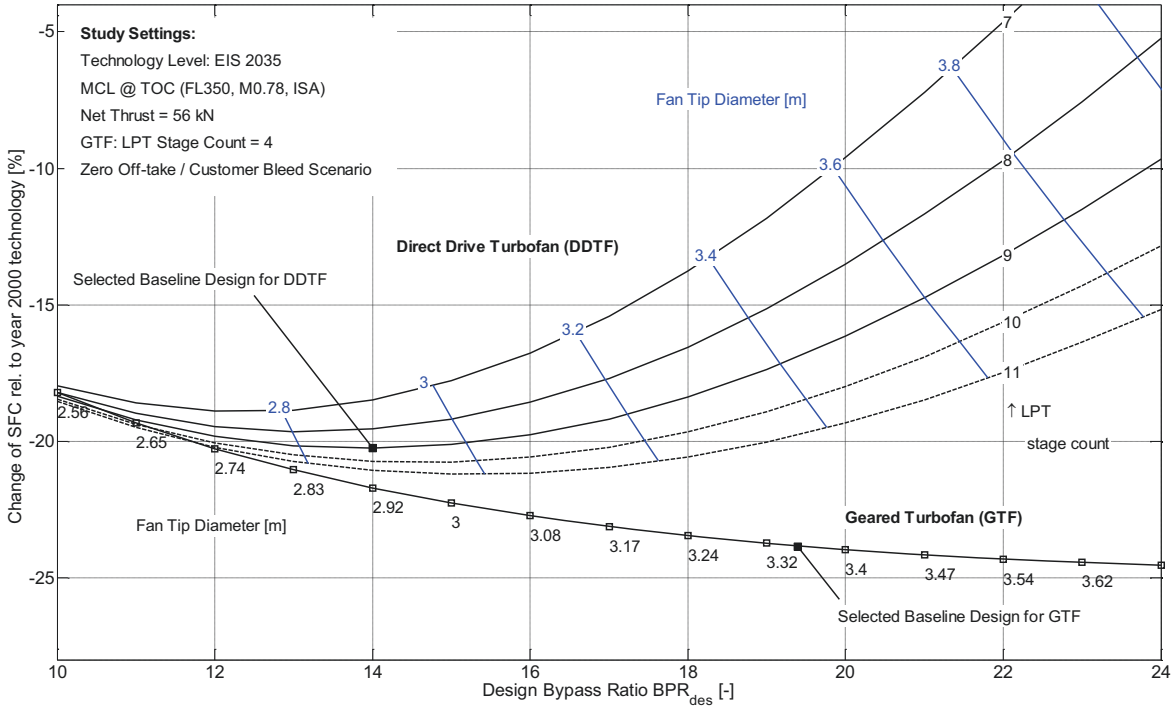

BILD 5 Impact of design Bypass Ratio on SFC for analyzed DDTF and GTF designs

efficiencies are slightly different due to variations of involved component efficiencies. As described above, the transmission efficiency of the GTF is penalized due to the reduced fan pressure ratio.

The obtained values for SFC correspond to an improvement of 20.3% and 23.9% relative to the year 2000 technology status. This appears to be consistent with the investigation performed in [21], in which 20% SFC improvement for a GTF with a BPR of 18.0 and a year 2025 technology status was calculated.

The designs described in TAB 4 may be considered as best and balanced considering the isolated power plants and is therefore denoted as 'baseline design'. However, when it comes to the assessment of vehicular performance, i.e. if also weight and drag implications are taken into account, the selected Bypass Ratios might not necessarily match the respective fuel burn optimum ones. Thus, the baseline designs provide a basis for subsequent investigation of the integration effects discussed in Section 4.

TAB 4: Synopsis of propulsion system design parameters for DDTF and GTF (baseline design)

	DDTF	GTF	Delta [a]
Engine Architecture			
	3-spool DDTF SDSF Nacelle	2-spool GTF SDSF Nacelle	
Stage Configuration			
Fan	1	1	
IPC/Booster	8	3	
HPC	6	9	
HPT	1	2	
IPT	2	n/a	
LPT	9	4	
Engine Size			
Fan Inlet Diameter [m]	2.89	3.35	+15.9
Performance at Max. Climb Point			
Operating Condition	M0.78, FL350, ISA		
F_N [kN]	56.0		
BPR_{des} [-]	14.0	19.4	+38.6
$F_N/W_{2,des}$	112.0	83.0	-25.9
OPR [-]	60.0		
TET [K]	1750		
Gear Ratio [-]	n/a	4.0	n/a
SFC [g/s/kN]	13.27	12.67	-4.5
ΔSFC rel. to Year 2000 Technology [%]	-20.3	-23.9	-3.6 [b]
η_c [-]	0.607	0.609	+0.2 [b]
η_{tr} [-]	0.832	0.826	-0.6 [b]
η_{pr} [-]	0.806	0.849	+4.3 [b]

[a] GTF relative to DDTF [%]
[b] Percentage points

4. DESIGN IMPLICATIONS AT AIRCRAFT LEVEL

In order to additionally account for the effects associated with power plant installation, a simplified analysis was conducted aiming at the identification of the most feasible engine option for the investigated application. The objective of this study was to observe the impact of variations of BPR_{des} on the change of aircraft block fuel relative to the initially selected baseline design summarized in TAB 4. Essential cycle characteristics and power plant component efficiencies were kept constant as defined above. After describing the modeling approach of the weight and drag impact, the characteristics of both engine architectures are compared to each other, and, suitable design points are identified and discussed.

4.1. Modeling of weight and drag implications

When considering vehicular cascade effects, the benefit of a SFC reduction obtained from a reduction of specific thrust is gradually counteracted by several effects: Since an increase in BPR_{des} at a given thrust yields a larger fan diameter, the weight of the fan assembly including the LP system and the nacelle tends to increase, too. Moreover, a larger nacelle diameter yields a larger wetted area leading to increased drag. As a further cascade effect, the landing gear height may need to be increased in order to provide sufficient nacelle ground clearance and to account for nose wheel collapse scenarios. Therefore, trade factors intended to capture the main implications of propulsion system installation were derived from the evolutionary improved medium to long range aircraft analyzed in Reference [10].

For the assessment of power plant component weights, the method introduced by Seitz [14] was utilized. Accordingly, the length and mass of each turbo component was calculated in a stage-wise manner. Stationary turbo component weights such as casings, vanes and additional structural elements were considered to be proportional to component annular volume. Rotating turbo component weights such as disks, blades and hub structures were treated proportional to the displaced volume, exhibiting sensitivity to the AN^2 metric and material specific strength. In view of the advanced technology standard considered in the present studies, for the fan a material specific strength was chosen corresponding to a mix of 80% Carbon Fiber Reinforced Polymers and 20% titanium. For the remaining turbo components, typical materials were selected. Hub to tip and aspect ratios appropriate for the considered applications were derived from References [11], [22] and [23]. The mass of the fan drive gear system was estimated according to a correlation given in Reference [24], which was calibrated to reflect the advanced technology status. The mass of bearing support structures, shafts, combustors, ducts and accessories was parametrically scaled according to information given in literature and in-house assessment. Nacelle component and equipment masses were estimated based on a method described in Reference [14].

For evaluating the relative variation of nacelle skin friction drag, it was assumed that drag primarily scales with nacelle wetted area and that this area may be approximated by a cylindrical surface shell, in the first

instance. For the parametric mapping of nacelle shaping, a set of empirical methods was employed. The nacelle diameter, D_n, was described using an empirical model applicable to mixed and separate flow turbofans, which was derived based on data given in References [25-30] including both the characteristics of existent engines and projected power plants featuring UHBPR. The correlation obtained from nonlinear regression follows a hyperbolic approach and exhibits sensitivity to the fan diameter, D_2:

$$\frac{D_n}{D_2} = \frac{0.28}{D_2} + 1.17 \quad (4)$$

The correlation is considered to be valid for fan diameters between 1.0 m and 3.5 m. All used data points were found to be within a +/- 5% confidence interval. A visualization of the implemented model is given in BILD 6.

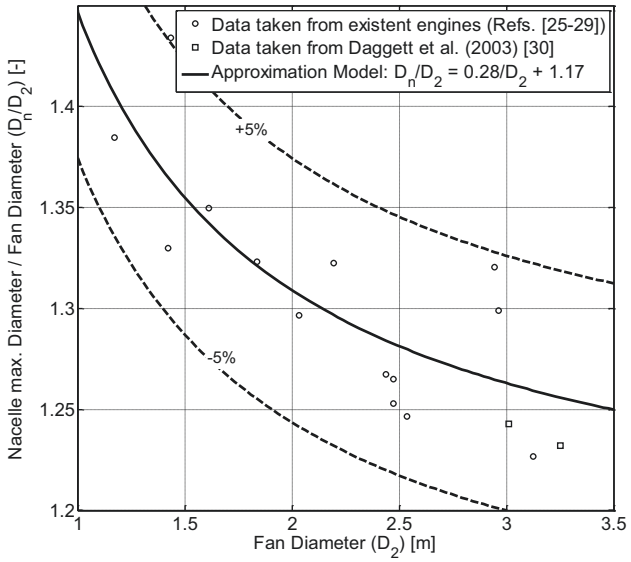

BILD 6: Implemented nacelle diameter model

Nacelle length was modelled using the correlation given in Reference [14], in which the nacelle length to diameter ratio, L_n/D_n, was found to be primarily dependent on fan outer pressure ratio, p_{13}/p_2:

$$\frac{L_n}{D_n} = 0.95 \cdot \frac{p_{13}}{p_2} - 0.09 \quad (5)$$

4.2. Results for the DDTF

BILD 7 shows the individual implications of the considered effects for varying BPR as well as the combined impact emanating from the combination of these effects for the DDTF. As can be seen, the LPT efficiency variation and its implication on SFC increasingly outweigh the gain of propulsive efficiency obtained from rising BPR. It can be observed that if the almost linearly increasing drag and weight implications are taken into account, the design that solely minimizes SFC is no longer the optimum solution. At aircraft level, the initial assumption of BPR_{des} = 14.0 was apparently selected slightly too high since minimum fuel burn is achieved with a BPR_{des} of 13.0. However, the relative benefit is only minor. A further increase of BPR leads to a rapid increase of block fuel and is therefore not desirable.

This simplified analysis indicates that with a direct drive configuration and under the imposed assumptions higher BPR are unlikely to yield improvements in fuel burn. Since apart from SFC, propulsion system weight has the highest impact on the change of block fuel, weight reducing technologies constitute a significant lever for shifting the fuel burn optimum to even higher BPR.

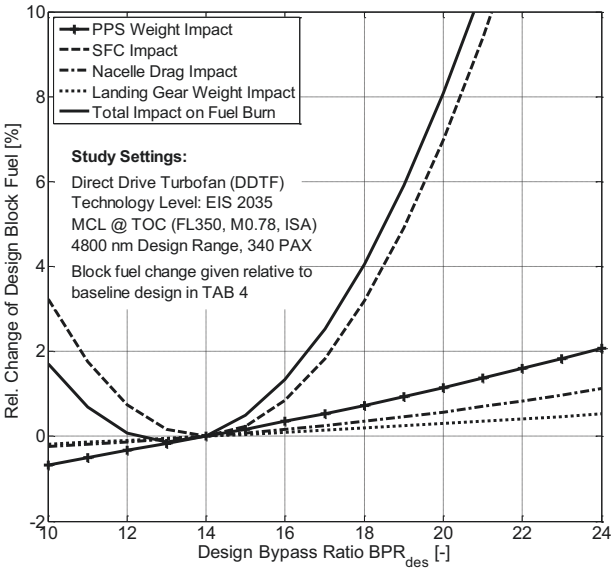

BILD 7: Impact of weight, drag and SFC on design block fuel as a function of BPR_{des} for DDTF design

BILD 8 presents the impact of LPT stage count on the change of design block fuel as a function of BPR_{des}. Under the given boundary conditions the maximum permissible stage count of 9 does not only yield optimum SFC but also minimum fuel burn. Similar to the SFC characteristics presented in BILD 5, the optimum Bypass Ratio is shifted to higher values for increasing stage counts. Due to the weight impact, a further increase of stage count increasingly compromises the corresponding SFC benefit. This result confirms the selection of 9 LPT stages, since a higher value only yields modest benefits but a substantial increase in part count, complexity and maintenance effort.

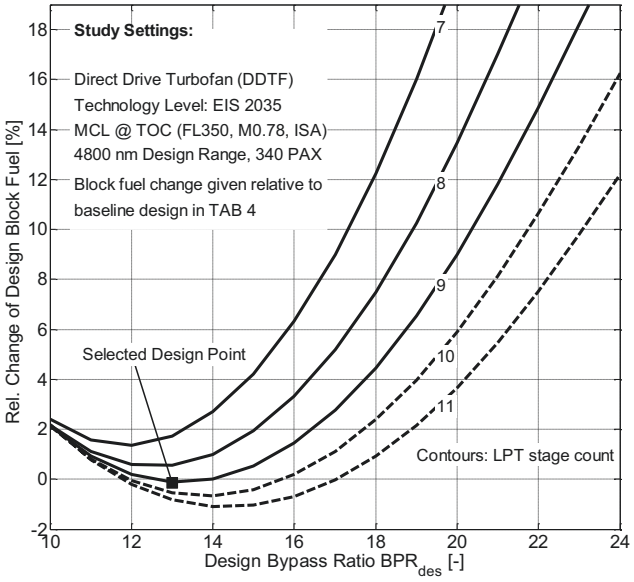

BILD 8: Impact of LPT stage count on block fuel for DDTF design

4.3. Results for the GTF

Subsequently, a similar study was conducted for the GTF. In BILD 9 the trade study results of the individual vehicular effects are displayed for the GTF.

As opposed to the DDTF, the SFC monotonically decreases with rising Bypass Ratios due to the ability of the engine architecture to maintain an almost constant LPT mean stage loading, which prevents the LPT efficiency from degrading for higher values of BPR. This behavior has a strong impact on the overall block fuel change characteristic as indicated in the figure. The fuel burn-optimum Bypass Ratio is reached with a value of approximately 23.0.

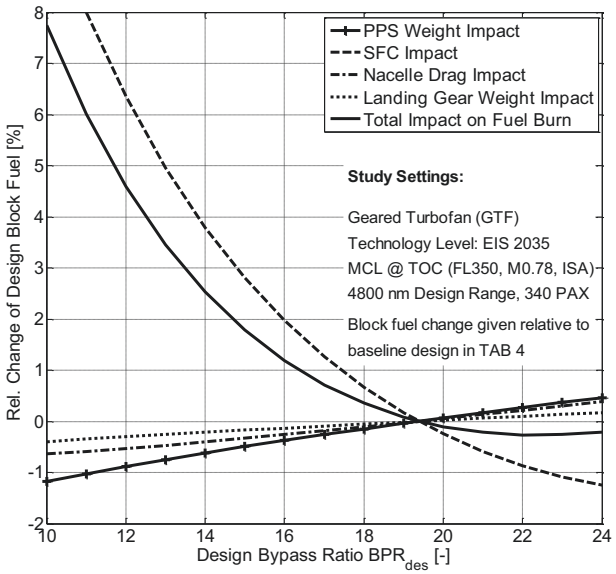

BILD 9: Impact of weight, drag and SFC on design block fuel as a function of BPR_{des} for GTF design

4.4. Comparison of Installed Performance

The previously discussed results were condensed into one comparative diagram (BILD 10) presenting the relative change of design mission block fuel for a wide range of design BPR for the DDTF and GTF relative to the baseline design of the GTF. Moreover, the respective fan diameters are annotated. Although in this study the impact of landing gear length increase for rising fan diameters was considered, the chart may also be conveniently used to gain a first idea of the possible improvement potential for re-engining purposes of existent aircrafts. In that case, since the landing gear typically remains fixed, the improvement potential, depending on the installation space available, might even be slightly higher than indicated in the figure.

As mentioned before, for the DDTF the minimum block fuel burn is obtained using BPR_{des} = 13.0. For the GTF, the identified minimum is shifted towards higher BPR values featuring an absolute block fuel minimum at BPR_{des} = 23.0. The fuel saving potential is again penalized for higher Bypass Ratios. However, the increase is much less significant as for the DDTF which is mainly driven by two effects: The ability of maintaining a constant LPT stage loading with rising BPR and the associated impact on SFC, which is superimposed by the resulting implication on the power plant weight trend. As according to the used exchange rates the SFC has the highest impact on fuel burn, the trend of converging SFC curves is propagated to the fuel burn characteristics and causes both trends to approach each other towards the lower end of BPR investigated.

Due to the flat nature of the fuel burn characteristic of the GTF in the vicinity of its minimum, one would in practice probably select a slightly lower BPR_{des} than the minimum one. This is driven by the fact that e.g. the improvement in fuel burn between the baseline design and the fuel burn minimum is 0.25 percentage points, while the latter engine design would require an 8.1% larger fan diameter. The associated increase in manufacturing and maintenance costs would need to be traded against a possible reduction in noise emissions. As an initial approach, for the GTF the baseline design using BPR_{des} = 19.4 was considered a best and balanced tradeoff between fuel efficiency and complexity, while for the DDTF the fuel burn-minimum value of 13.0 was selected. With these design settings the GTF features a 4.7% lower SFC relative to the DDTF. As a consequence of the significantly reduced specific thrust level and corresponding mean nozzle exit velocity, there is initial indication that noise emissions are reduced for the selected GTF design relative to the DDTF. In view of similar temperature and pressure levels, no significant differences in NOx emissions are expected for both power plant options, in the first instance. The DDTF exhibits a fuel burn penalty of 5.5% relative to the GTF.

TAB 5: Synopsis of propulsion system design parameters for selected design

	DDTF	GTF	Delta [a]
Engine Size			
Fan Inlet Diameter [m]	2.79	3.35	+20.1
Performance at Max. Climb Point			
Operating Condition	M0.78, FL350, ISA		
F_N [kN]	56.0		
BPR_{des} [-]	13.0	19.4	+49.2
F_N/W_2 [m/s]	119.7	83.0	-30.7
OPR [-]	60.0		
TET [K]	1750		
Gear Ratio [-]	n/a	4.0	
SFC [g/s/kN]	13.29	12.67	-4.7
ΔSFC rel. to Year 2000 Technology [%]	-20.1	-23.9	-3.8 [b]
η_c [-]	0.607	0.609	+0.2 [b]
η_{tr} [-]	0.843	0.826	-1.7 [b]
η_{pr} [-]	0.795	0.849	+5.4 [b]
Integrated Characteristics			
Total PPS Weight [kg]	7774	7648	-1.6
Nacelle Wetted Area [m^2]	39.1	48.2	+23.3
Δ Block Fuel rel. to GTF [%]	+5.5	±0.0	
Δ Block Fuel rel. to Year 2000 Technology [%]	-26.7	-32.2	

[a] GTF relative to DDTF [%]
[b] Percentage points

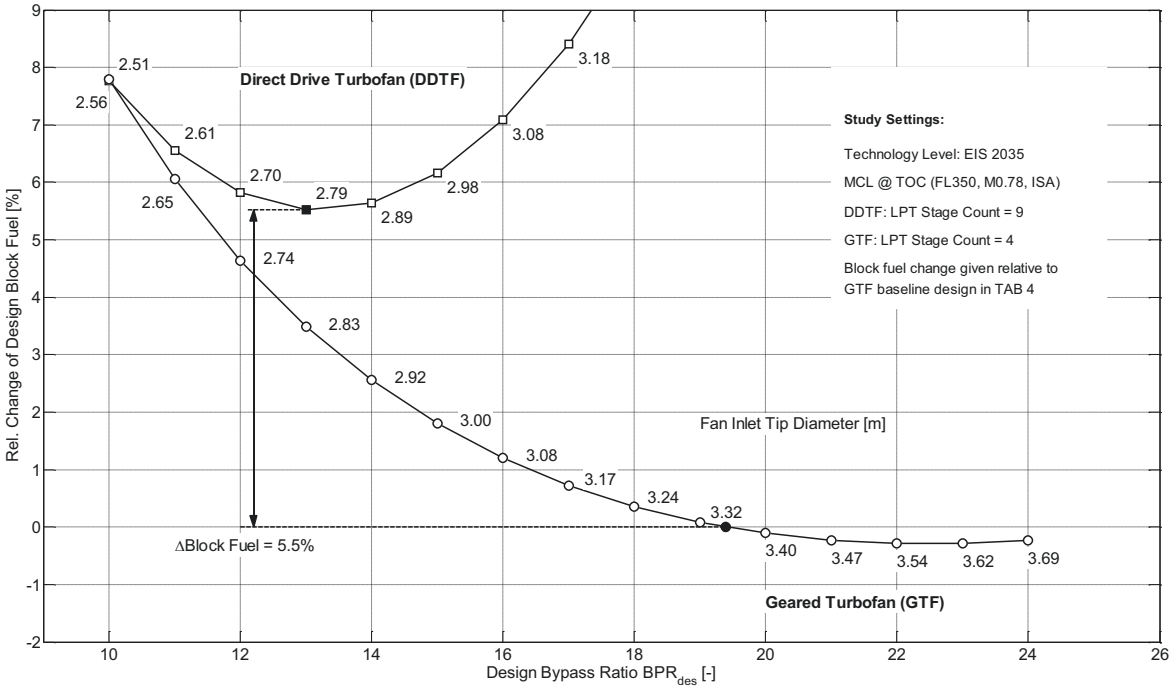

BILD 10: Comparison of fuel burn change for selected DDTF and GTF propulsion concepts

The advanced aircraft described in Section 2.1 equipped with the GTF power plants of the selected design features a 32.2% block fuel reduction relative to the year 2000 technology status. Hence, the aircraft powered by the selected DDTF design would yield a 26.7% reduction in fuel burn. A summary of further design parameters is presented in TAB 5.

As a consequence of the increased fan diameter of the GTF, the nacelle wetted area is significantly larger for the GTF although it is counteracted by the nacelle length to diameter ratio, which tends to become smaller with decreasing fan pressure ratios. The gear ratio required for the given BPR increases to a value of 4.0, which was considered to be achievable using a single-stage planetary reduction gear system.

At the selected design conditions the GTF features a 1.6% lower propulsion system weight and a 7.3% lower bare engine weight compared to the DDTF. The weights of important component groups are given in TAB 6. The increased number of stages for both HPC and HPT yields a substantially increased HP spool system weight for the selected GTF design. Moreover, the GTF benefits from the complete shortfall of the IP spool system. The LP spool system comprises the weights of the fan assembly, an optional fan drive gear system and the LPT including associated shafts and bearing supports. As can be seen, the increased weight of the fan and the reduced LPT weight nearly cancel each other out. In detail, it was found that due to the lower fan tip speed associated with the reduced fan pressure ratio of the GTF the increase in weight emanating from the greater fan volume is counteracted by alleviated centrifugal stress. Similarly, the weight improvement of the LPT caused by reduced stage count is penalized by increased rotational speed. The nacelle group includes the weights of the inlet, engine mounts, C-duct, thrust reverser and nozzle assemblies. As most nacelle items are sensitive to fan size, the GTF suffers from a nacelle weight penalty.

TAB 6: Comparison of component group weights

Weight Item	Delta [a] [%]
HP Spool System [b, c]	+146.6
IP Spool System	-100.0
LP Spool System [b, e]	-4.0
Nacelle	+20.9
Bare Engine Weight [d]	-7.3
Total Propulsion System Weight [f]	-1.6

[a] GTF relative to DDTF
[b] including turbo components, shafts and bearing support
[c] including combustor
[d] including fan case mounted accessories
[e] in case of GTF including booster and fan drive gear system
[f] including operating fluids

In summary, it is recognized that there are significant differences in the loci of fuel burn optimum BPR for both investigated engine architectures. The fuel burn reduction potential exhibited with the GTF relative to the baseline design is higher than the one achievable with the DDTF. For moderate values of BPR the differences tend to diminish and both engine options appear to be feasible. However, if the full range of UHBPR is exploited, the GTF seems to be the most appropriate architecture.

As also stated in References [8] and [9], a major advantage of the GTF is associated with a significant reduction of part count, specifically regarding the LPT. While not explicitly considered in the context of this paper, this would be an indication for lower manufacturing and maintenance cost. As was found in the present studies, at the design points selected the GTF is characterized by an almost neutral total power plant weight compared to the DDTF despite a significantly increased fan diameter.

The derived trends generally agree with results published in the past. For example, References [30] and [31], in which similar medium to long range applications were considered, found the fuel burn optimum BPR to be located at lower values for a DDTF than for a GTF and the

respective fuel burn benefit to be higher for the GTF. In Reference [30] the values for optimum BPR were 11.5 and 14.3, respectively and thus lower than found in the present investigation, thereby illustrating the dependence of the results on the implemented technology level. While Reference [30] assumed year 2015 as a technology readiness date, the present studies focused on a 2035+ EIS. The associated component efficiency improvement yields smaller core sizes, thus leading to increased BPR at a constant fan diameter.

5. CONCLUSION AND FURTHER WORK

This paper focused on the comparative assessment of two evolutionary improved Ultra-High Bypass Ratio (UHBPR) turbofan engines for an entry-into-service of year 2035+, which may be used for benchmarking purposes against highly advanced unconventional propulsion systems potentially available in the same timeframe. These propulsion system options comprised a three-spool Direct Drive Turbofan (DDTF) and a Geared Turbofan (GTF).

From an initial study, which considered the evaluation of isolated propulsion system performance in terms of specific fuel consumption (SFC) for a broad range of design Bypass Ratios (BPR), it was found that for the DDTF the characteristics of SFC strongly depend on the number of installed Low Pressure Turbine (LPT) stages, as this determines the mean stage loading and thus LPT efficiency. While for the DDTF the minimum SFC was sensitive with the number of LPT stages employed, the SFC of the GTF showed to continuously decrease with reducing levels of specific thrust within the considered range of BPR investigated.

In order to additionally capture the effects of propulsion system weight and drag, a trade factor based study was conducted aiming on the identification of fuel burn optimum design values of BPR. It was found that for the DDTF the fuel burn optimum BPR was slightly dislocated to lower values than for the uninstalled case featuring an optimum BPR of 13.0. For higher BPR, the DDTF became increasingly unattractive due to the increasing impact of power plant weight and wetted area. For the GTF, the optimum value was found to be 23.0, mainly a result of its specific characteristics of SFC and weight change with BPR. Moreover, the fuel burn characteristic of the GTF was rather flat in the vicinity of its optimum, thus motivating the use of a slightly smaller BPR and fan diameter without suffering excessive penalties but possibly yielding lower costs. The improvement in block fuel burn relative to year 2000 technology status was 26.7% and 32.2% for the DDTF and the GTF, respectively. The total propulsion system weight of the GTF was found to be almost neutral compared to the DDTF (-1.6%), although the GTF offered a 20.1% greater fan diameter allowing eventually for the realization of significantly reduced specific thrust levels and thus improved propulsive efficiency.

It has to be noted that the location of the optimum BPR and the relative improvement potential depends on the assumptions imposed, in particular regarding the technology level and associated component efficiencies as well as the block fuel exchange rates for SFC, drag and weight that were employed. Moreover, apart from the fuel burn improvement potential, fan size and specific thrust levels might also be dictated by noise targets leading to designs that not necessarily coincide with the fuel burn optimum ones. Similarly, the design might also be driven by cost and complexity implications not considered within this paper, which could possibly shift the selected BPR to lower values.

A future refined study should take into account more detailed implications of UHBPR engines on the integrated aircraft sizing process. As large engine diameters yield increased windmilling drag, this especially includes appropriate sizing of the vertical tail in order to maintain yaw control under minimum controllable conditions during one-engine-inoperative scenarios. Therefore, an integrated aircraft and propulsion system assessment should be conducted to allow for more detailed modeling of further vehicular cascade effects, and to investigate e.g. the sensitivity of optimum cruise speeds for aircraft using UHBPR. In addition, the potentials associated with the exploitation of variable engine geometries in the context of UHBPR such as an adaptable bypass nozzle should be analyzed.

6. ACKNOWLEDGEMENTS

The authors would like to thank Dr. Askin T. Isikveren for fruitful discussions and valuable advice, as well as Clément Pornet for providing the trade factors used in this paper.

7. REFERENCES

[1] European Commission, “Flightpath 2050: Europe’s Vision for Aviation”, Report of the High Level Group on Aviation Research, Publications Office of the European Union, Luxembourg, 2011

[2] Isikveren, A.T. (Bauhaus Luftfahrt e.V.), "Distributed Propulsion and Ultra-high By-pass Rotor Study at Aircraft Level (DisPURSAL)", FP7-AAT-2012-RTD-L0, Proposal No. 323013, European Commission Directorate General for Research and Innovation, March 2012.

[3] Baier, H. (Technische Universität München), “Morphing Enabling Technologies for Propulsion System Nacelles (MorphElle)”, FP7-AAT-2012-RTD-L0, Proposal No. 341509, European Commission Directorate General for Research and Innovation, October 2013

[4] von der Bank, R. (Rolls-Royce Deutschland GmbH), “Low EMissions COre-Engine TEChnologies (LEMCOTEC)”, FP7-AAT-2011-RTD-1, Proposal No. 283216, European Commission Directorate General for Research and Innovation, December 2010.

[5] Merkl, E. (MTU Aero Engines GmbH), “ENgine mOdule VAlidators (ENOVAL)”, FP7-AAT-2013-RTD-1, Proposal No. 604999, European Commission Directorate General for Research and Innovation, 2013

[6] Silva, M. (Turbomeca SA) “Engine BREAK-through components and sub-systems (E-BREAK)”, FP7-AAT-2012-RTD-1, Proposal No. 314366, European Commission Directorate General for Research and Innovation, December 2011

[7] Rao, A., (Technische Universiteit Delft) “Advanced Hybrid Engines for Aircraft Development (AHEAD)”, FP7-AAT-2011-RTD-1, Proposal No. 284636, European

Commission Directorate General for Research and Innovation, October 2011

[8] Kurzke, J., „Fundamental Differences between Conventional and Geared Turbofans“, Proceedings of ASME Turbo Expo 2009 Gas Turbine Technical Congress and Exhibition, Orlando, Florida, June 8-12, 2009, GT2009-59745

[9] Larsson, L., Avellán, R., Grönstedt, T., “Mission Optimization of the Geared Turbofan Engine”, ISABE, Gothenburg, 2011, ISABE-2011-1314

[10] Isikveren, A.T., Seitz, A., Bijewitz, J., Hornung, M., Mirzoyan, A., Isyanov, A., Godard, J.-L., Stückl. S., van Toor, J., „Recent Advances in Airframe-Propulsion Concepts with Distributed Propulsion“, paper no. 2014_0853, 29th Congress of the International Council of the Aeronautical Sciences, St. Petersburg, Russia, September 7-12, 2014

[11] Grieb, H., Schubert, H. (Ed.), “Projektierung von Turboflugtriebwerken“ Birkhäuser Verlag, Basel-Boston-Berlin, 2004

[12] Kurzke, J., GasTurb 11, Compiled with Delphi 2007 on 27 January, 2010

[13] Guynn, M., Berton, J., Tong, M., Haller, W., “Advanced Single-Aisle Transport Propulsion Options Revisited”, 2013 Aviation Technology, Integration, and Operations Conference, August 12-14, 2013, Los Angeles, California, AIAA 2013-4330

[14] Seitz, A., „Advanced Methods for Propulsion System Integration in Aircraft Conceptual Design”, PhD Dissertation, Institut für Luft- und Raumfahrt, Technische Universität München, 2012.

[15] Guha, A., „Optimisation of aero gas turbine engines“, The Aeronautical Journal, Vol. 105 (1049), pp. 345-358, July 2011

[16] Gauntner, J., “Algorithm for calculating turbine cooling flow and the resulting decrease in turbine efficiency”, NASA Technical Memorandum, Lewis Research Center, Cleveland, Ohio, February 1989, NASA-TM-81453

[17] Münzberg, H.-G., Kurzke, J., „Gasturbinen – Betriebsverhalten und Optimierung“, Springer-Verlag New York Heidelberg Berlin, 1977

[18] Kurzke, J., “Achieving maximum thermal efficiency with the simple gas turbine cycle”, 9th CEAS European Propulsion Forum: “Virtual Engine – A Challenge for Integrated Computer Modelling”, Rome, Italy, October 15-17, 2003

[19] Rolls-Royce website, www.rolls-royce.com, 01.05.2014

[20] Seitz, A., Schmitz, O., Isikveren, A. T., Hornung, M., „Electrically Powered Propulsion: Comparison and Contrast to Gas Turbines”, Deutscher Luft- und Raumfahrt Kongress (DLRK), Berlin, Germany, September 10-12, 2012

[21] da Rocha-Schmidt, L., Hermanutz, A., Baier, H., Seitz, A., Bijewitz, J., Isikveren, A.T., Scarpa, F., Allegri, G., Remillat, C., Feuilloley, E., Majić, F., O’Reilly, C., Efraimsson, G., “Progress Towards Adaptive Aircraft Engine Nacelles”, paper no. 2014_0770, 29th Congress of the International Council of the Aeronautical Sciences, St. Petersburg, Russia, September 7-12, 2014

[22] Whurr, J., “Future Civil Aeroengine Architectures and Technologies”, 10th European Turbomachinery Conference, Lappeenranta, Finland, April 15-19, 2013

[23] Kappler, G., Staudacher, S., “Gewichtsstudie zu Niederdrucksystemen moderner Turbofan-Triebwerke”, Deutscher Luft- und Raumfahrt Kongress (DLRK), Berlin, Germany, September 10-12, 2012

[24] Reynolds, C., "Advanced Propfan Engine Technology (APET) Single- and Counterrotation Gearbox / Pitch Change Mechanism, Final Report", Pratt & Whitney United Technologies Corporation, NASA-CR-168114, Vol. 1 & 2, 1985

[25] Daly, M., Gunston, B., “IHS Jane’s Aero Engines 2013/2014”, 2013

[26] A320 - Airplane Characteristics for Airport Planning. Airbus S.A.S., 31707 Blagnac Cedex, France, May 2014

[27] A330 - Airplane Characteristics for Airport Planning. Airbus S.A.S., 31707 Blagnac Cedex, France, January 2014

[28] A340 - Airplane Characteristics for Airport Planning. Airbus S.A.S., 31707 Blagnac Cedex, France, January 2014

[29] A380 - Airplane Characteristics for Airport Planning. Airbus S.A.S., 31707 Blagnac Cedex, France, December 2013

[30] Daggett, D., Brown, S., Kawai, R., “Ultra-Efficient Engine Diameter Study”, Boeing Commercial Airplane Group, Seattle, Washington, May 2003, NASA/CR-2003-212309

[31] Howe, D., Wyonosky, T., “Energy Efficient Engine Program – Advanced Turbofan Nacelle Definition Study”, United Technologies Corporation Pratt & Whitney Engineering Division”, May 1985, NASA CR-174942